

Article ID: 1006-8775(2014) 01-0074-13

ANALYSIS OF EFFECT OF ENVIRONMENTAL POTENTIAL VORTICITY LOCATED AT SOUTH EDGE OF SOUTH ASIA HIGH ON INTENSIFICATION OF TROPICAL CYCLONES

DING Zhi-ying (丁治英), XING Rui (邢蕊), XU Hai-ming (徐海明), GAO Yong (高勇)

(Key Laboratory of Meteorological Disasters of the Ministry of Education (Nanjing University of Information Science & Technology), Nanjing 210044 China)

Abstract: The NCEP $1^\circ \times 1^\circ$ reanalysis of June-to-September dataset between 2002 to 2009 is used in this study to conduct statistical analysis of the relationship between the environmental potential vorticity (PV) on 150 hPa located at the south edge of South Asia High (SAH) and TCs making landfall. The results show that 23 of the TCs are affected by the PV on 150 hPa located at the south edge of SAH between 2002 to 2009, and three TCs' center pressure decline after the high-value environmental PV moves to the center of the TCs. These three TCs are Senlaku (0216), Bilis (0604) and Linfa (0903). Through diagnostic analysis from the viewpoint of isolines, we determined the relationship between the intensification of these TCs and the PV anomaly at high levels; the isentropic surface is close to the high level's PV anomaly under the influence of the 150-hPa PV anomaly, leading to the decline of isentropic surfaces on both sides of the PV anomaly. Then the warm core of the middle and high levels of the TC strengthens and PV increases at the middle level, and both of them are beneficial to the reinforcement of the cyclonic vorticity in the low level. As a result, the center pressure of the TC declines. According to Wu's theory of Slantwise Vorticity Development (SVD), the incline of the isentropic surfaces leads to the development of vertical vorticity, contributing to the vertical motion and the release of the latent heat. Then the warm core of the TC strengthens and the TC strengthens, too. Otherwise, piecewise PV inversion also shows that the high-level PV influences the mid-level more than the low level.

Key words: potential vorticity (PV); intensification of TCs; South Asia High (SAH); Slantwise Vorticity Development (SVD); PV inversion

CLC number: P444 **Document code:** A

1 INTRODUCTION

The middle-latitude system is transporting energy to the low latitude through large-scale tilted troughs in westerlies. The energy will have important effects on tropical cyclones (TCs), and one of the ways is potential vorticity^[1, 2, 3], or PV for short. Early in the 1930s to 1940s, Rossby^[4] and Ertel^[5] proposed the concept of PV and proved that it conserves. In recent decades, the PV and its application became widely known at home and abroad. From the viewpoint of PV, the atmospheric structure can be cyclonic and anticyclonic around the positive and negative PV in upper levels, as well as around the positive and negative potential temperature in low levels. According to the PV theory, the upper part is known as PV sink. The PV theory is often used to explain the

formation and development of a cyclone. For example, through diagnostic analysis of the excessive Meiyu front rainstorm that appeared in Yangtze-Huaihe (YH) area in summer, Wu and Shou^[6] put forward that latent heat release will prompt downward transmission of the high PV in upper levels, resulting in the development of the cyclone in low levels, and discussed a possible mechanism for the development of a YH cyclone.

PV that is conveyed to low latitudes contains energy not only from the middle latitude but also from the stratosphere. In summer, over China and the area to its east, South Asia High is very strong and the energy transported to the south will propagate along its peripheral flow. Sometimes the energy transmitted downward will encounter the TC moving northward,

Received 2013-01-16; **Revised** 2013-10-25; **Accepted** 2014-01-15

Foundation item: National Key Fundamental Research Development Program Planning "973" (2009CB421503; 2013CB430103); Natural Science Foundation of China (41375058); Construction of Advantageous Disciplines for Higher Education in Jiangsu Province; Priority Academic Program Development of Jiangsu Higher Education Institutions (PAPD)

Biography: XING Rui, M.S., primarily undertaking research on mesoscale meteorology.

Corresponding author: DING Zhi-ying, e-mail: dingzhiying@nuist.edu.cn

flow into the center of TC in upper levels, and further have impact on its intensity. Early in 1998, based on the complex influence on TC intensity by synoptic scale troughs in the troposphere, Molinari et al.^[7] analyzed the interaction between the TC Danny (1985) and the positive PV anomaly in the upper troposphere through PV analysis and proposed the principle of superposition, that is, the superposition of the small-scale positive upper PV anomaly with the TC center in low levels can intensify the TC, based on the research findings of E-P flux, vertical wind shear and the interaction between diabatic and vortex. In this study, results from diagnostic analysis and PV inversion are used to explain the influence of upper PV on TC intensity when the upper PV located on the south of SAH flows into the TC center on the low levels. The global final (FNL) analysis dataset with a horizontal resolution of $1^\circ \times 1^\circ$ provided by the National Centers for Environmental Prediction (NCEP) is adopted in this work.

2 PV FLOWING INTO TC CENTER AND STRENGTHENING OF TC

By using FNL dataset in June, July, August and September from 2002 to 2009, a statistical analysis on PV on the upper levels and 41 TCs that landed in the Chinese mainland revealed that 23 out of the 41 TCs are influenced by PV located on the south edge of South Asia High at 150 hPa. When a large PV (more than 2 PVU) at 150 hPa is located in the area within 500 km from the border of the closed circulation of TCs at 850 hPa, it indicates that the PV influence is evident. The phenomenon that the PV on upper levels coincides with the TC center in the lower troposphere only occurs in 7 out of 23 TCs—4 of them in the late period of TCs—and does not play a role in the intensification of TCs. For the remaining 16 TCs, the influence is not clear. The center pressure of 3 TCs decreases when the large PV located on the south edge of South Asia High moves into the TC center before it reaches its maximum intensity. The 3 TCs are Sinlaku (0216), Bilis (0604), and Linfa (0903). The process in which the environmental PV located at the south edge of South Asia High moves into the TC center can be seen from Fig. 1. Fig. 2 exhibits that after the large PV coincides with the TC center at low levels, the three TCs intensify significantly and reach their maximum strength.

3 CROSS-SECTIONAL ANALYSIS OF POTENTIAL TEMPERATURE

According to the PV theory^[1], if the value of PV larger than the surrounding in the positive PV anomaly region exists in upper air, the vorticity and static stability will be both large in this region and the

surfaces of equipotential temperature gather together around the positive PV anomaly center, and then lead to the increase of the distance between adjacent surfaces of equipotential temperature above and below the positive PV anomaly, and the static stability reduces. Following the law of PV conservation, the cyclonic vorticity enlarges and cyclonic circulation is generated around the positive PV anomaly. Considering the close relationship between the equipotential temperature surface and the positive PV anomaly in upper air, the analysis of the potential temperature field is as follows. Fig. 3 is the pressure-time section of potential temperature averaged on a $6^\circ \times 6^\circ$ square area. It can be seen from Fig. 3a that for TC Sinlaku the isentropic surface changes little with time from the very beginning to 0000 UTC 30 August 2002 for the whole levels of TCs. After 0000 UTC 30 August, large environmental PV on upper levels begin moving into the TC center, and then the isentropic surfaces tilt downward evidently at high levels above 350 hPa until 0000 UTC 1 September, and the pressure of the TC center decreases to minimum. The isentropic surfaces tilt again at 1200 UTC 4 September but not very significantly. Together with Fig. 2, it can be seen that the isentropic surfaces tilt obviously after the upper environmental PV coincides with the TC center at low levels. Meanwhile the decreasing speed of pressure in the TC center suddenly accelerates and the TC reaches its maximum intensity. The pressure of the TC center declines mildly as the isentropic surfaces tilt later (at about 1200 UTC 4 September).

The time evolution of the isentropic surfaces above 300 hPa for TC Bilis (0604) is different from that of Sinlaku. For the initial time at 0000 UTC 9 July 2006, the isentropic surfaces at high levels tilt downward, but high-level large PV does not show up until 0000 UTC 13 July and the isentropic surfaces tilt downward obviously until 0600 UTC 14 July. The isentropic surfaces tilt upward at 1800 UTC 14 July. Together with Fig. 2b, it can be found that the pressure is falling down without the appearance of large PV at high levels before 0000 UTC 13 July. Although the downward tilting of isentropic surfaces is conducive to the TC intensification, not all the inclining of isentropic surfaces is caused by PV anomalies at high levels. The isentropic surfaces incline downward further when the large PV at high levels moves into the TC center at about 0000 UTC 13 July, then the pressure of the TC center drops further and the TC reaches its maximum intensity. The TC becomes weaker when the isentropic surfaces stop tilting downward and start to incline upward.

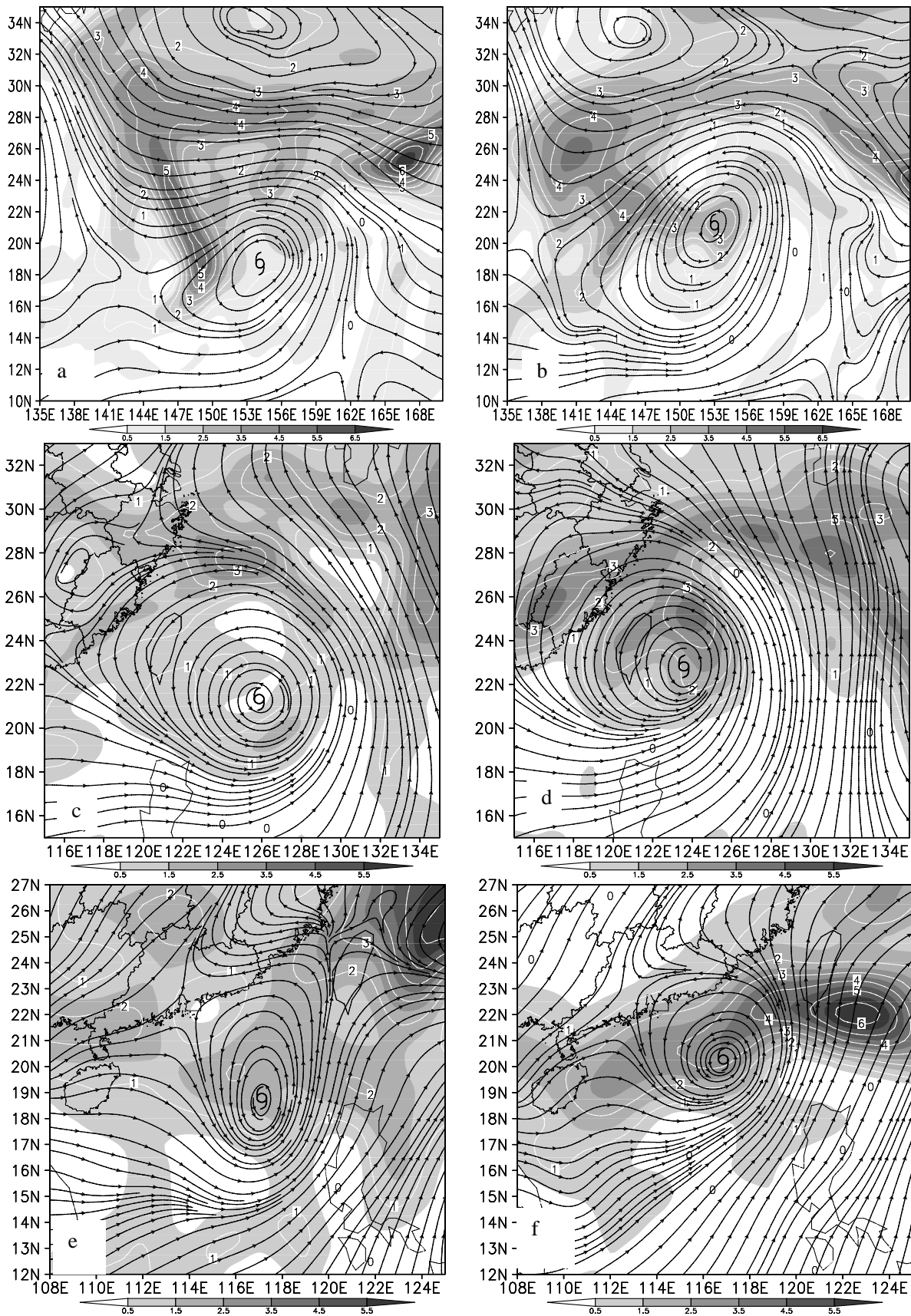


Figure 1. Horizontal plot of potential vorticity (shaded) at 150 hPa and flow field (streamline) at 850 hPa. (a, b): 1200 UTC 29 and 0600 UTC 30 August for Sinlaku; (c, d): 0000 UTC 12 and 0000 UTC 13 July for Bilis; (e, f): 0000 UTC 19 and 0000 UTC 20 June for Linfa, with the interval of PV at 1 PVU.

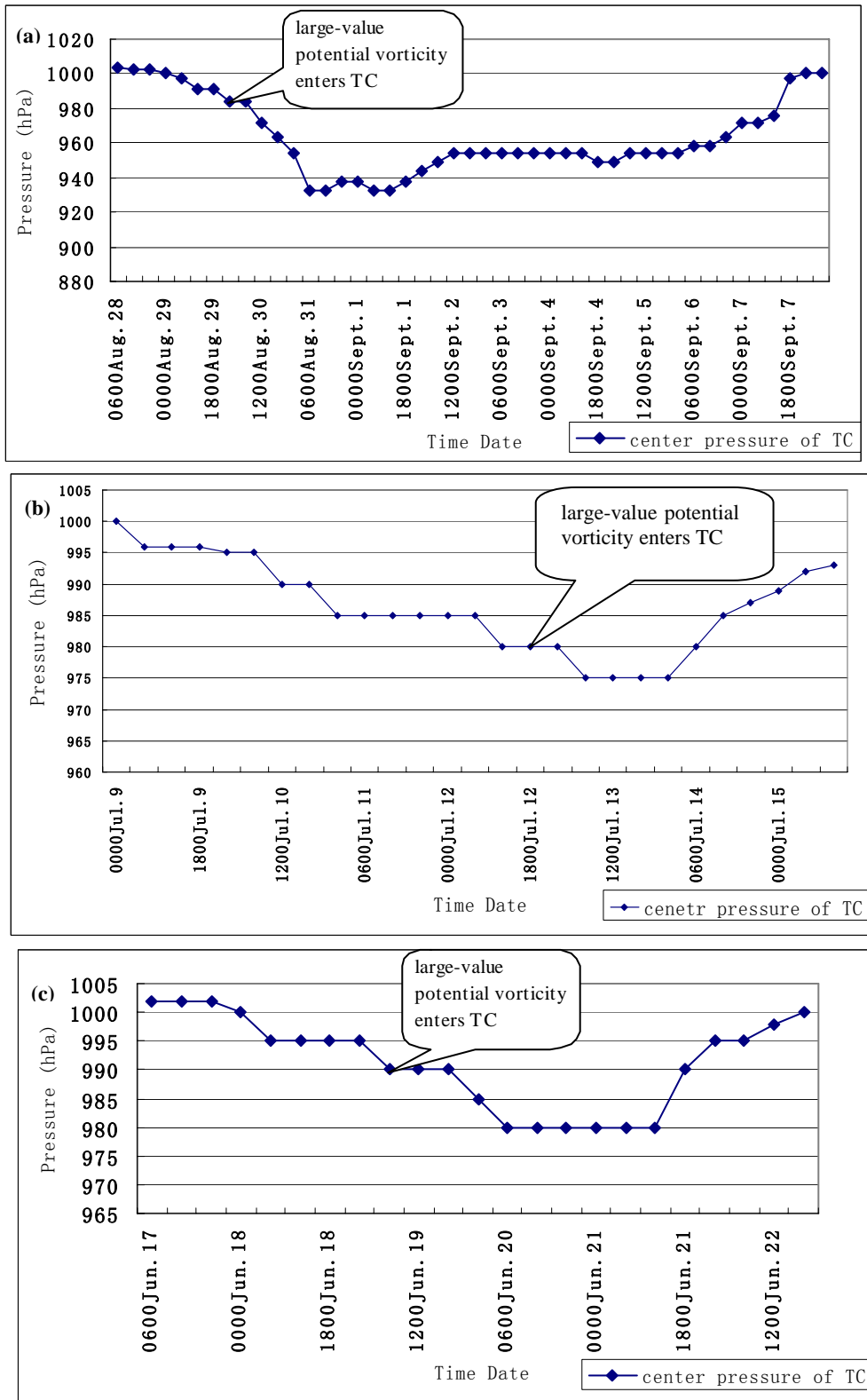


Figure 2. Time series of the pressure in the TC center of (a) Senlaku, (b) Bilis, and (c) Linfa.

As for TC Linfa (0903, see Fig. 3c), the process is similar to that of Sinlaku. In detail, the isentropic surfaces are smooth and change little above 300 hPa before the environmental PV moves into the TC center. It starts to incline downward obviously at 0000 UTC 20 June 2009 after the environmental PV in

upper air moves into the TC center. Then the isentropic surfaces stop tilting downward and incline upward until 1800 UTC 21 June. Together with Fig. 2, it is shown that a drop in the pressure of the TC center continues and the TC reaches its maximum intensity after the large PV in the upper troposphere moves into

the TC center. Besides, the pressure increases when the isentropic surfaces start to incline upward.

Based on the analysis of the pressure-time cross section of potential temperature for these 3 TCs, it is suggested that there is obvious relationship between the environmental PV and the downward tilting of isentropic surfaces. The equipotential temperature surface begins to tilt downward after the upper large environmental PV moves into the TC center, then the pressure drops quickly or continues to fall to the

minimum. However, for some TCs, the isentropic surfaces start to tilt downward from the very beginning and will incline downward further when the large PV moves into the TC center. When the isentropic surfaces tilt upward, the depression damps with the weakening of the TC. As shown in Fig. 3, the isentropic surfaces can incline downward to 500 hPa to produce a warm core above it, which facilitates the development and maintaining of the TC.

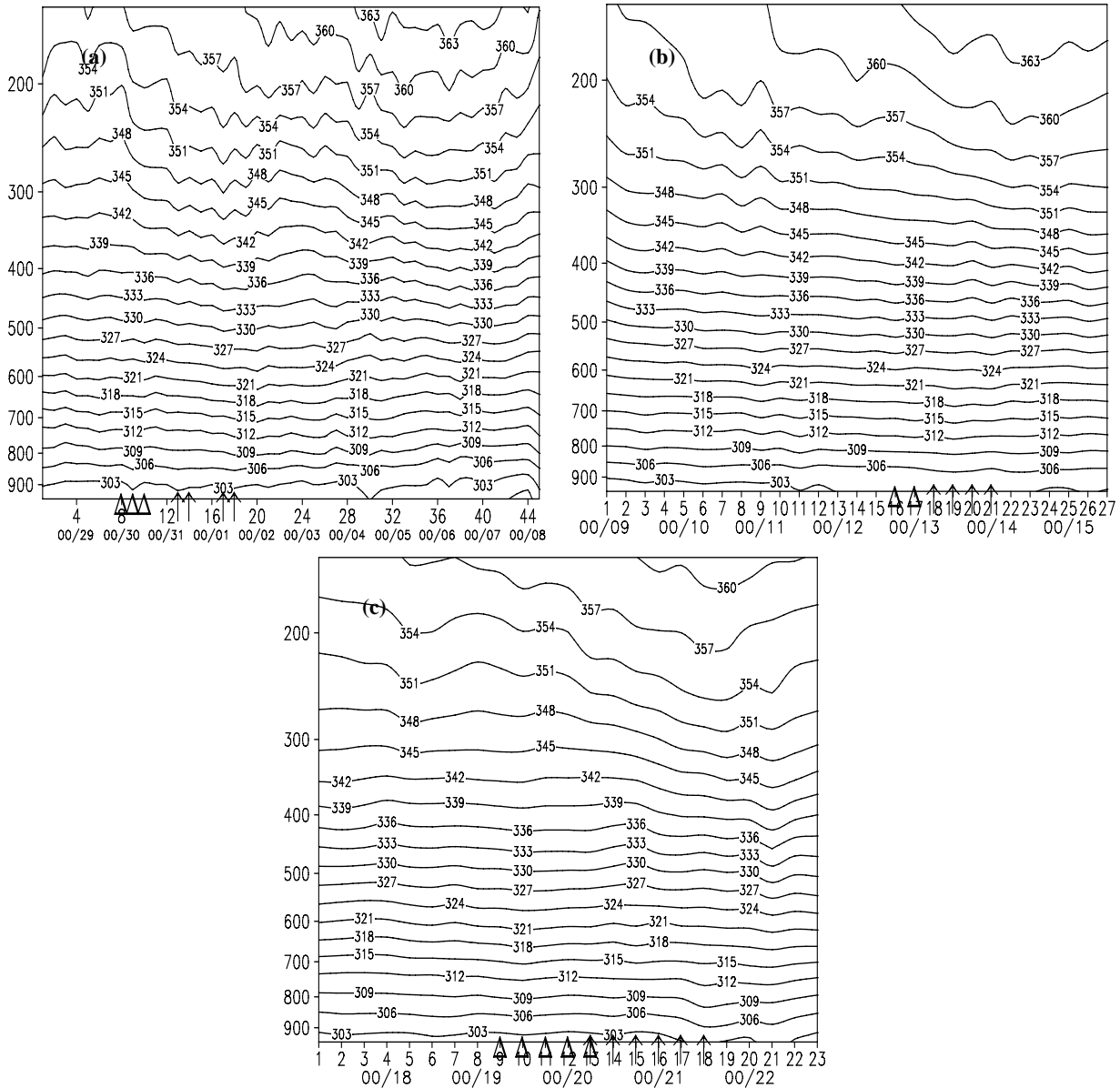


Figure 3. Pressure-time cross sections of potential temperature for (a) Senlaku, (b) Bilis, and (c) Linfa. The interval is 3 K, the hollow triangle symbol indicates the time when the TC center is overlaid by large PV, and the upward arrow denotes the time when TC reaches its maximum intensity.

The analysis of Fig. 4 (the zonal circulation along the TC center after the large PV moves into it) is described as follows. A large positive PV area corresponding to the TC center (20°N, 152°E) at 850 hPa is in the upper troposphere on 0000 UTC 30

August (Fig. 4a). The isentropic surfaces below the large PV converge to it and tilt upward, inducing the isentropic surfaces on the eastern side of the large PV center to incline downward. In addition, the downward sloping region is corresponding to the

ascending. Therefore, the downward sloping of isentropic surfaces favors the intensification of the TC. In Fig. 4a, the downward tilting of isentropic surfaces is related to the large PV in the middle and lower troposphere. It can also be seen from Fig. 4b that the several large PV centers on 150 hPa are situated in the center of Bilis (23°N, 124°E), and the isentropic surfaces merge into the PV centers and then tilt downward. Thus the TC develops rapidly in this period and the warm core appears near the TC center, so that the isentropic surfaces tilt downward more

obviously than the counterpart of Senlaku. The downward tilting area on the middle and lower levels is also corresponding to the positive PV anomaly. Note that the isentropic surfaces are more likely to incline downward between the two large PV regions on high levels and are likely to intensify the warm core if the TC is located in that region. The downward invasion of isentropic surfaces also favors the ascending and the formation of positive PV and cyclonic vortex on middle and low levels. This is also true for Linfa (Fig. 4c).

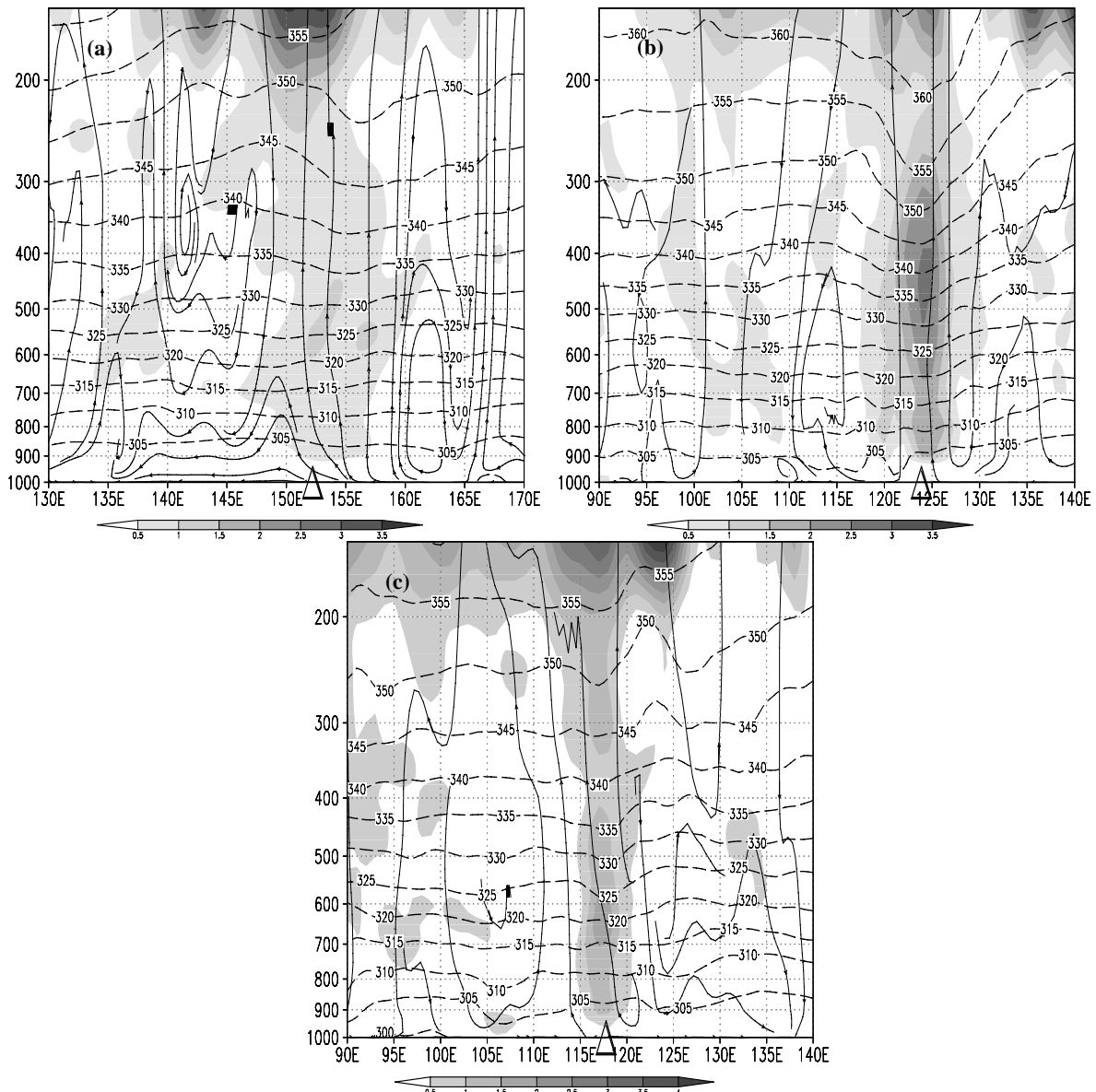


Figure 4. Zonal circulation along the TC center as large PV moves into it (omega is enlarged by 10 times and the hollow triangle symbol denotes the TC center). The shading and contour are for the PV (shaded, PVU) and potential temperature (dotted line, K), respectively. (a): Sinlaku, 0000 UTC 30 August 2002, along 20°N; (b): Bilis, 0000 UTC 13 July 2006, along 23°N; (c): Linfa, 0000 UTC 20 June 2009, along 21°N.

The intensification of a TC is associated with the formation of the warm core structure^[8] and based on the above analysis, the upper large PV can produce the downward tilting of isentropic surfaces on both

sides, which facilitates the formation of the warm core in the TC and strengthens it. The factors favoring the intensification of TCs are described as follows. Fig. 5 is the time series of the averaged difference of

perturbation temperature between the mean temperature in the square area of $2^{\circ} \times 2^{\circ}$ and the area of $6^{\circ} \times 6^{\circ}$, whose centers are around the eye of the TC respectively. As for Sinlaku (Fig. 5a), the perturbation temperature greater than 0.4°C on upper levels appears after the upper PV moves into the TC center. Subsequently, as the TC strengthens, the perturbation temperature increases gradually. The large perturbation temperature is all above 400 hPa when the TC reaches its maximum intensity. The center of large perturbation temperature develops downward in the maintenance period (from 0000 UTC 4 September to 0000 UTC 7 September) and the warm center disappears gradually during the decaying phase (after 0000 UTC 7 September). Large perturbation temperatures are located on the middle levels in the initial stage of Bilis (Fig. 5b). The upper perturbation

temperature increases after the upper large PV moves into the TC center and the TC reaches its maximum intensity. The situation of Linfa is similar (Fig. 5c), i.e., positive perturbation temperatures on upper levels increase after the upper-level large PV moves into the TC center and the TC reaches its maximum intensity.

Changes in the temperature structure of the eyes of these three TCs also confirm the conclusions mentioned above. Based on the theory of Slantwise Vorticity Development in Wu et al.^[9-11], the declination of the isentropic surfaces can result in the enhancement of vertical vorticity, so that the vortex is more likely to develop in the declination area of the isentropic surfaces. Thus the convection is strengthened by the vortex development to release latent heat, which is conducive to the intensification of the warm center in the TC.

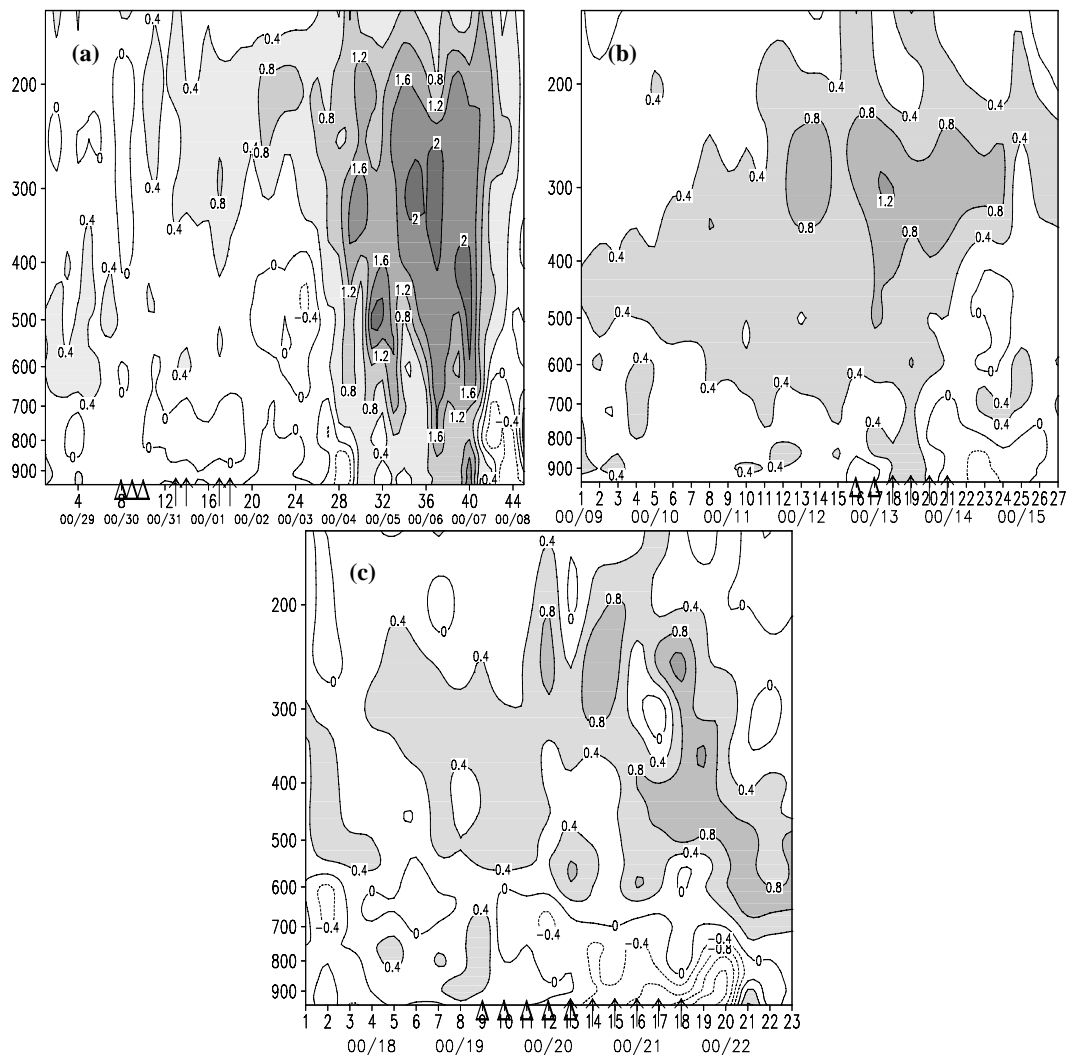


Figure 5. Pressure-time cross sections of the thermal perturbation for (a) Sinlaku, (b) Bilis, and (c) Linfa. The interval is 0.4°C . The hollow triangle symbol and the upward arrow have the same meaning as in Fig. 3.

4 CROSS SECTION OF PV AND VORTICITY

The evolution of middle and upper PV can lead to the development of the lower vortex and the vorticity

increment^[12]. On the basis of them, we analyzed the relationship between the PV and the vorticity near the TC center.

Figure 6 depicts the pressure-time cross section of

PV averaged in the square area of $6^{\circ} \times 6^{\circ}$ centered in the TC eye. It can be found that the mid- and lower-level PV increases obviously after the upper PV moves into the eye of the TC, then the pressure of the TC center reaches its minimum. Two large positive PV areas usually exist in the development stage of the TC, one above 200 hPa and the other around 500 hPa. Large PV on upper levels is usually corresponding to the development of PV on middle levels, while changes in PV of these three TCs are different. As for Sinlaku (Fig. 6a), the PV is enhanced first above 200 hPa and stretches downwards slightly. The PV between 250 hPa and 700 hPa increases to 0.8 PVU after upper PV moves into the TC center and then to 1.0 PVU as the TC reaches its maximum intensity. The PV maximum of more than 1.8 PVU on middle levels appears around 1200 UTC 4 September in the late stage of TC development. However, the situation

of Bilis is different from that of Sinlaku (Fig. 6b). In the initial time, the PV on middle levels already reaches 0.8 PVU and increases gradually. The PV on upper levels is 0.8 PVU on 0000 UTC 12 July, then increases gradually and moves into the TC center. The PV between 500 hPa and 300 hPa increases to 1.6 PVU (that is the maximum) after the upper PV moves into the eye of TC and the TC reaches its maximum intensity at the same time. By analyzing the PV evolution of Linfa (Fig. 6c), it can be found that the PV between 700 hPa and 200 hPa increases significantly (from 0.6 PVU to 0.8-1.0 PVU) from 1200 UTC 19 June after the upper PV moves into the TC center. The PV on upper levels first reaches its maximum of more than 1.4 PVU, and then the PV on middle levels increases to its maximum of 1.0 PVU and the pressure in the TC center decreases to the minimum simultaneously.

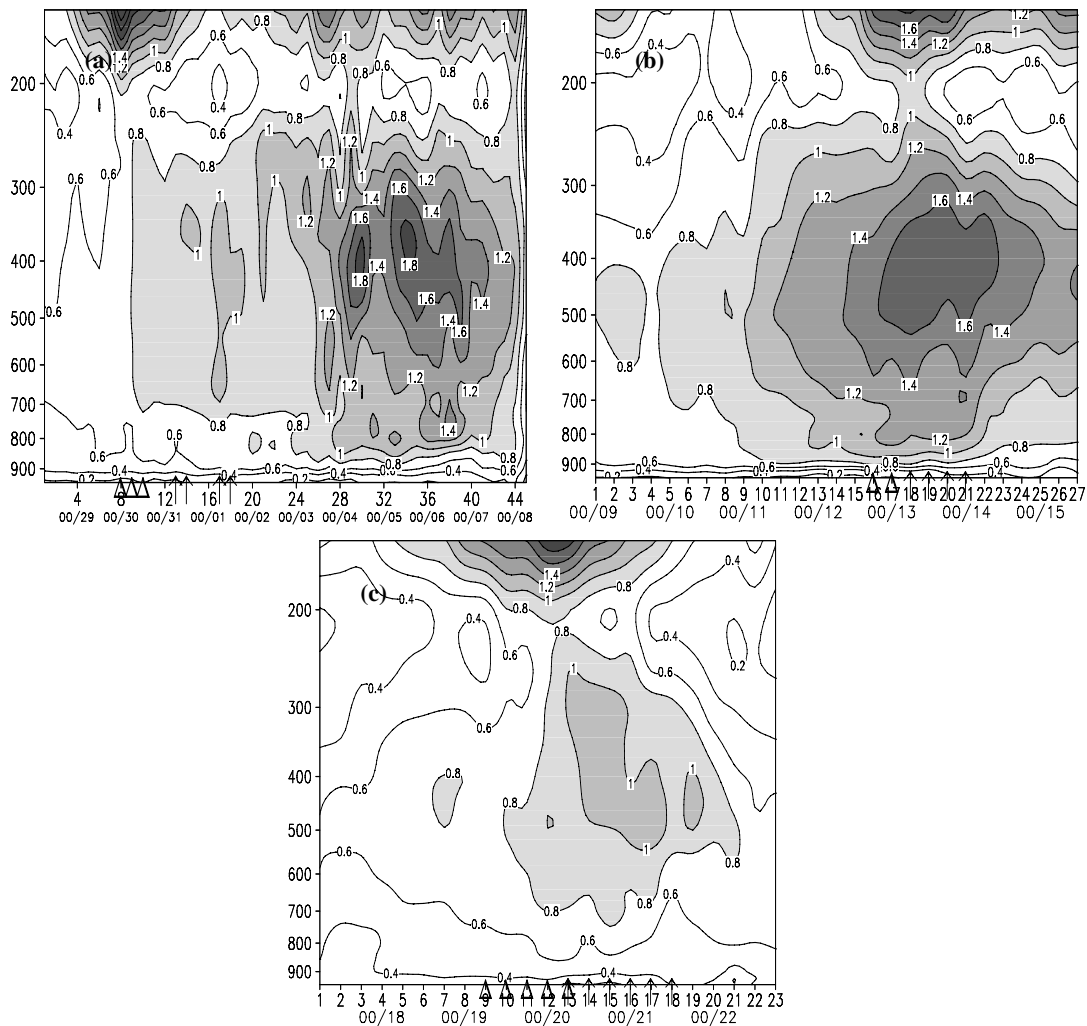


Figure 6. Pressure-time cross sections of PV for (a) Sinlaku, (b) Bilis, and (c) Linfa. The interval is 0.2 PVU. The hollow triangle symbol and the upward arrow have the same meaning as in Fig. 3.

According to the above analysis, for Sinlaku and Linfa, the PV on middle levels develops substantially and increases to maximum gradually after the upper PV moves into the TC center. For Bilis, the PV on

middle levels increases gradually at first, and then reaches its maximum after the upper PV moves into the TC center.

Figure 7 is the pressure-time section of relative

vorticity averaged in the square area of $6^{\circ} \times 6^{\circ}$ which is centered around the eye of TC. Taking Sinlaku (Fig. 7a) for example, the PV on middle levels increases significantly after the upper large PV moves into the TC eye, then the relative vorticity increases substantially between 950 hPa and 400 hPa. The vorticity increases from $5 \times 10^{-5} \text{ s}^{-1}$ to $6-7 \times 10^{-5} \text{ s}^{-1}$ and then the pressure in the TC center decreases to the minimum. The maximum vorticity reaches $12 \times 10^{-5} \text{ s}^{-1}$ around 0000 UTC 6 September. Compared with the section of PV (Fig. 6a), it can be found that vorticity maximum at low levels increases after the PV maximum appears on middle levels, and the PV on middle levels develops without the environmental upper PV moving into the eye of TC after 0000 UTC 3 September. At this moment, Fig. 7a presents that the cyclonic vorticity on the middle and low levels increases dramatically, which indicates that the positive PV on middle levels are conducive to the development of lower positive vorticity favoring the

TC maintenance. Comparison of the cross section of vorticity (Fig. 7b) with that of PV (Fig. 6b) for Bilis shows that the PV maximum appears first on middle levels between 550 hPa and 350 hPa as the upper PV moves into the TC center. Afterwards, the lower positive vorticity enhances continuously with the vorticity maximum occurring at low levels between 900 hPa and 750 hPa. Lower vorticity strengthens as the PV on middle levels intensifies continuously, indicating the important effect of PV at middle levels on the vorticity at low levels. The positive environmental PV on the upper air moves into the TC center, encouraging the development of TC. After large PV moves into the center of Linfa (Fig. 7c), the PV on the middle troposphere develops to strengthen the lower-level vorticity. At the same time, the pressure in the TC center reaches its minimum, and the process is similar to that of the two TCs mentioned above.

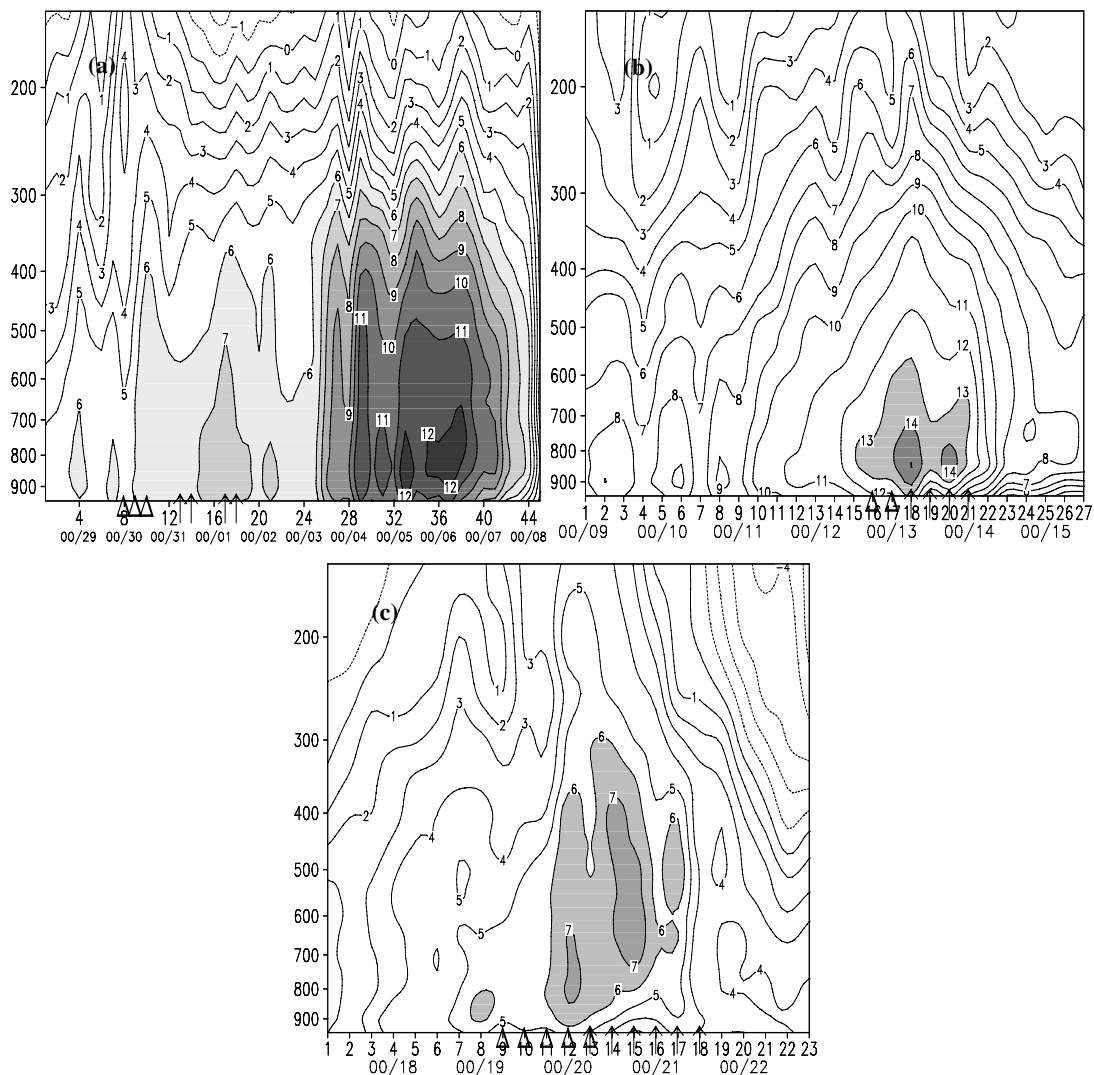


Figure 7. Pressure-time cross sections of relative vorticity for (a) Sinlaku, (b) Bilis, and (c) Linfa. The interval is 1 and the unit is $1 \times 10^{-5} \text{ s}^{-1}$. The hollow triangle symbol and the upward arrow have the same meaning as in Fig. 3.

Above all, mid-level PV develops dramatically or continuously to reach its maximum after the

upper-level environmental PV moves into the TC center, while the development of mid-level PV can enhance the lower-level cyclonic vortex, i.e., the TC intensification. Based on the PV theory, the positive PV anomaly in the upper troposphere can induce cyclonic circulation and stretch downward (the stretching scale is the Rossby penetrating height) to produce the vorticity and to increase the mid-level PV. Similarly, the positive PV anomaly on middle levels can result in cyclonic circulation and stretch downward to enhance the lower-level vorticity.

5 PIECEWISE PV INVERSION

Another important characteristic of PV is that it is inversable^[1, 13, 14]. The PV inversion indicates that the PV and nonlinear balance condition construct an equation set expressed by PV (indicated by q), geopotential field ϕ and stream function ψ . If one knows the distribution of PV and certain boundary conditions, the geopotential field and stream function will be calculated to derive wind, pressure and temperature. Partial PV inversion indicates that PV can be decreased, increased and broken up arbitrarily. The contribution to the whole stream field by local

perturbation is confirmed through inverting PV anomaly. Thus, the separation of PV perturbation on upper levels can confirm its effect on TC. Taking Senlaku for example, this study uses the partial PV inversion by Davis^[14] and the National Centers for Environmental Prediction (NCEP) global final (FNL) analysis dataset with the horizontal resolution of $1^\circ \times 1^\circ$.

The experiment design is as follows: experiment I is to remove the PV perturbation on middle and low levels and to reserve upper-level PV perturbation at 350-100 hPa. Experiment II is to reserve the PV perturbation on middle and low levels and to remove half of the upper-level PV perturbation at 350-100 hPa. A control experiment is to reserve the PV perturbation at all levels. The comparison of the inversed results based on the control experiment and real-time data are shown in Fig. 8. Comparison of the inversed stream field with the observed one on 850 hPa implies that major synoptic systems on 850 hPa can be determined through the Davis inversion of PV and the results are identical to the observation only with some difference in detail. Therefore, the data is reliable to some extent.

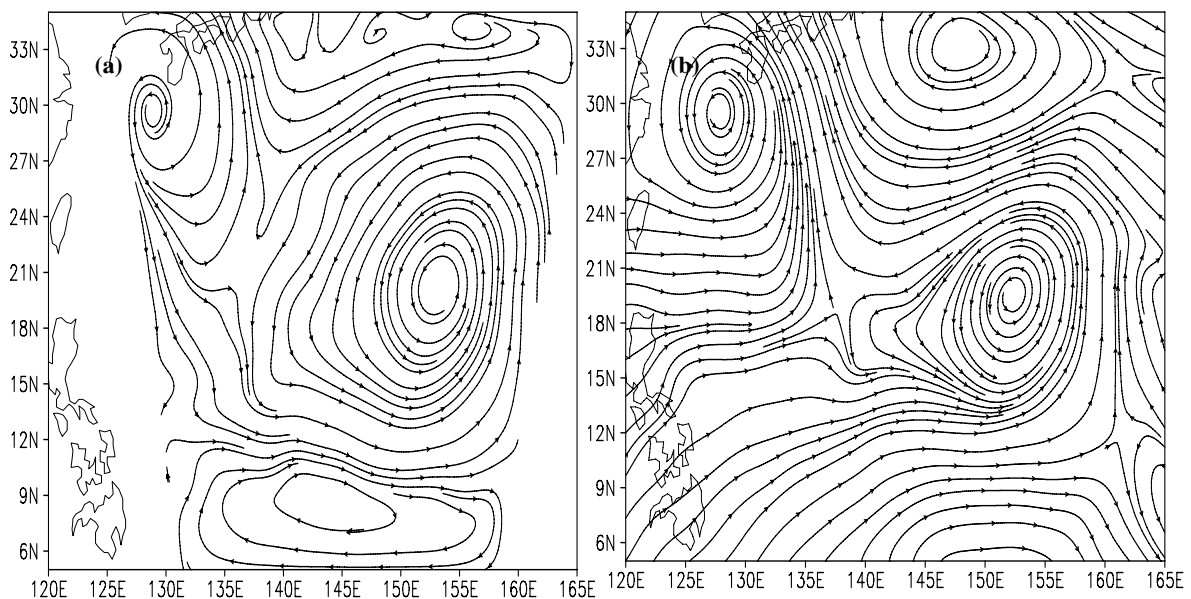


Figure 8. Horizontal plot of stream fields for Sinlaku calculated with PV inversion in the control experiment (a) and the observation (b) on 850 hPa at 0000 UTC 30 August.

The compared results of geopotential height fields on 500 hPa in experiment I and control experiment are depicted in Fig. 9a and 9b. It can be seen that in the control experiment the position of TC center on 500 hPa is similar to that in experiment I with weaker TC intensity. The TC center in the control experiment (Fig. 9b) is located at (150-155°E, 21-24°N) at 1200 UTC 30 August with the center geopotential height at 5680 gpm, while the TC center in experiment I (Fig. 9a) on 500 hPa is similar to that in the control

experiment and the center intensity is 5820 gpm, which is 140 gpm more than that in the control experiment. This implies that the TC circulation on 500 hPa can be obtained via reserving the upper-level PV perturbation, which facilitates to the strengthening of the TC on middle levels.

The results of geopotential height field on 850 hPa compared between experiment I and control experiment are shown in Fig. 9c and 9d. The results show that the position of TC center on 850 hPa in the

control experiment is generally the same as that on 500 hPa, and the position of TC center in the control experiment on 850 hPa is similar to that in experiment I with weaker TC intensity. TC intensity in the control experiment is about 1280 gpm on 1200 UTC 30

August, while being about 1480 gpm in experiment I. It demonstrates that the influence of the upper-level PV perturbation on the TC intensity in the middle troposphere is stronger than that in the lower troposphere.

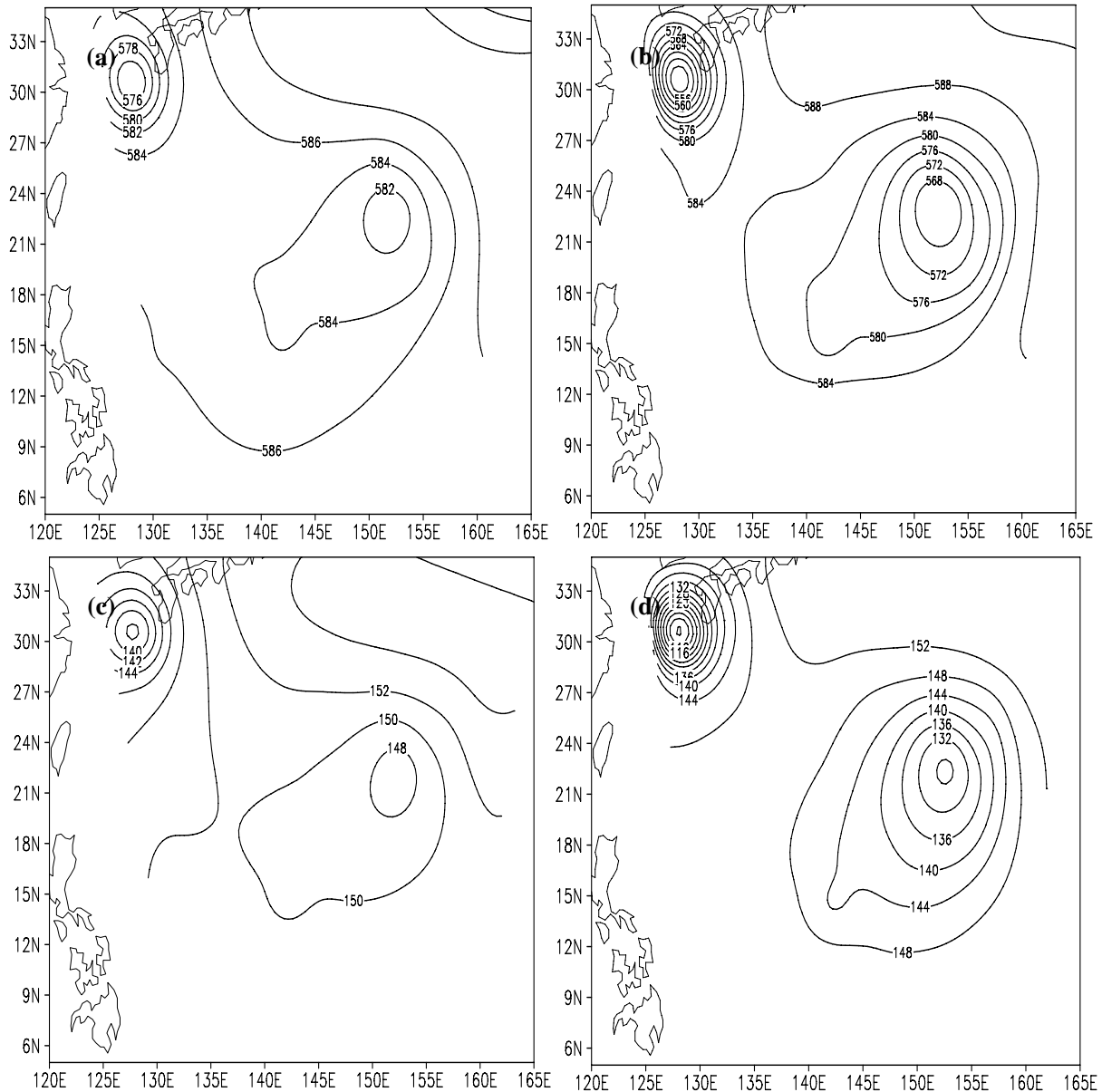


Figure 9. Horizontal plots of geopotential height fields (unit: geopotential meter $\times 10$) at 500 hPa (a, b) and 850 hPa (c, d) of Sinlaku in experiment I (a, c) and control experiment (b, d) at 1200 UTC 30 August 2002.

Figure 10 depicts the difference between experiment II and the control experiment. That is the difference in the 500 hPa and 850 hPa geopotential height fields between experiment II with 50% reduction of the upper-level PV perturbation and the control experiment. It can be found from Fig. 10 that the geopotential height with respect to the TC circulation increases in different degrees after the 50% reduction of the upper-level PV perturbation in the upper air at the position of TC circulation (150–155°E, 21–24°N) at 1200 UTC 30 August. At 500 hPa the

geopotential height increases by 14–18 gpm but by 6–8 gpm at 850 hPa. Similar results are obtained at other times (not shown). The result indicates that the TC becomes weak after reducing the upper-level PV perturbation, and from the PV inversion it can be concluded that the upper-level PV perturbation has positive contribution to the TC intensity on middle and low levels. Geopotential height increases by 8 gpm in the TC circulation on 850 hPa (Fig. 10b), which is much less than that on 500 hPa, indicating the stronger effect of upper-layer PV perturbation on

the mid-level TC circulation.

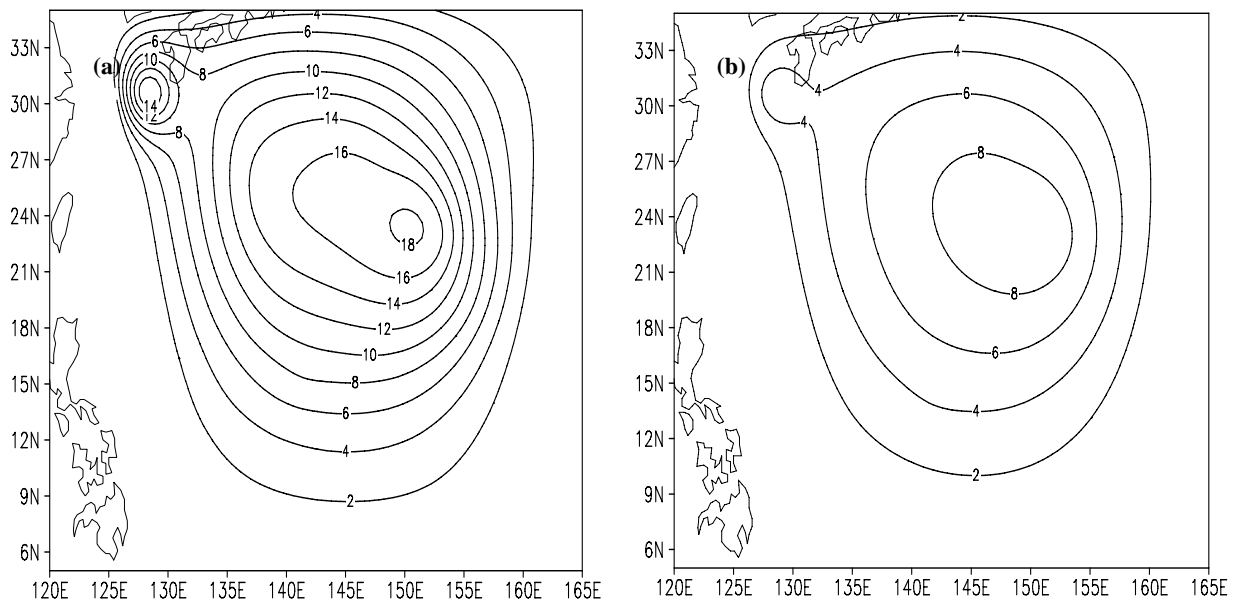


Figure 10. Difference of 500 hPa (a) and 850 hPa (b) geopotential heights (unit: geopotential meter) between experiment II and the control experiment at 1200 UTC 30 August 2002.

Geopotential height increases significantly on both 500 hPa and 850 hPa after 50% reduction of the upper-level PV perturbation when it moves into the TC center (not shown), while the effect becomes weak afterwards, illustrating that the upper-level PV moving into the TC center has significant effect on the TC intensity.

6 CONCLUSIONS

(1) A statistical analysis of upper-level PV of 41 TCs generated from 2002 to 2009 is performed in this work, and the results show that 23 of the TCs are affected by the PV on 150 hPa located on the south edge of SAH. The reason is that the energy transported to the lower latitudes through large-scale tilted troughs in the westerly can propagate along the border circulation of SAH. The center pressure in 3 of the 23 TCs declines significantly after the large environmental PV on the south edge of SAH moves into the TC center in the upper troposphere. These 3 TCs are Sinlaku (0216), Bilis (0604) and Linfa (0903), respectively.

(2) The isentropic surfaces will tilt after the large positive PV moves into the TC center to produce the strengthened warm center at the upper layers (200-300 hPa) of the TC. From the perspective of PV, the isentropic surfaces gather in the large positive PV area as they are influenced by the positive upper-level PV anomaly. Then the isentropic surfaces on both sides of the positive PV anomaly tilt downward to strengthen the warm center on middle and high levels and the mid-level positive PV. The enhanced warm center and positive PV on middle levels are favorable to the

cyclonic vorticity at lower levels, resulting in the decreased pressure in the TC center. Based on the theory of Slantwise Vorticity Development, possible reasons for the strengthening of the warm center in TC are concluded as follows. The declination of isentropic surfaces can enhance the vertical vorticity and the vortex, which is more likely to develop in the declination area of the isentropic surfaces. Then the convection is intensified by the developed vortex to release latent heat to intensify the warm center in TC. Based on the PV theory, the upper-level positive PV anomaly can induce a downward-stretching cyclonic circulation (with the stretching scale being Rossby penetrating height), which can increase the positive vorticity and the PV on middle levels. Similarly, the mid-layer positive PV anomaly can produce a downward-stretching cyclonic circulation to strengthen the lower vorticity.

(3) It is found through the PV inversion that the upper-layer PV perturbation can intensify the TC in the middle and lower troposphere and the effects are more significant to the middle levels than the lower levels.

REFERENCES:

- [1] SHOU Shao-wen, LI Shen-shen, SHOU Yi-xuan, et al. Mesoscale Meteorology [M]. Beijing: Higher Education Press, 2009: 273-281.
- [2] SHOU Shao-wen. Theory and application of potential vorticity [J]. Meteor. Mon., 2010, 36(3): 9-18.
- [3] HU Bo-wei. Some opinions about the potential vorticity thinking and its applications [J]. J. Nanjing Inst. Meteor., 2003, 26(1): 111-115.
- [4] ROSSBY C-G. Planetary flow patterns in the atmosphere

- [J]. *Quart. J. Roy. Meteor. Soc.*, 1940, 66: 68-87.
- [5] ERTEL H. Ein neuer hydrodynamischer Wirbelsatz [J]. *Meteor. Z.*, 1942, 59: 277-281.
- [6] WU Hai-ying, SHOU Shao-wen. Potential vorticity disturbance and cyclone development [J]. *J. Nanjing Inst. Meteor.*, 2005, 25(4): 510-517.
- [7] MOLINARI J, SKUBIS S, VOLLARO D, et al. Potential vorticity analysis of tropical cyclone intensification[J]. *J. Atmos. Sci.*, 1998, 55: 2632-2644.
- [8] DING Yi-hui. *Advanced Synoptic Meteorology* [M]. Beijing: China Meteorological Press, 2005: 278-284.
- [9] WU Guo-xiong, CAI Ya-ping, TANG Xiao-jing. Moist potential vorticity and slantwise vorticity development [J]. *J. Meteor.*, 1995, 53(4): 387-405.
- [10] WU Guo-xiong, LIU Huan-zhu. Complete form of vertical vorticity tendency equation and slantwise vorticity development [J]. *J. Meteor.*, 1999, 57(1): 1-15.
- [11] WANG Ying, WANG Yuan, ZHANG Li-xiang, et al. The development of slantwise vorticity near a weakened tropical cyclone [J]. *J. Trop. Meteor.*, 2007, 23(1): 47-52.
- [12] HOSKINS B J, MCINTYRE M E, ROBERTSON A W. On the use and significance of isentropic potential vorticity maps [J]. *Quart. J. Roy. Meteor. Soc.*, 1985, 111: 877-946.
- [13] ZHANG Shu-wen, WANG Shi-gong. Potential vorticity and potential vorticity inversion [J]. *Plateau Meteor.*, 2001, 20(4): 468-473.
- [14] CHRISTOPHER A. DAVIS. Piecewise potential vorticity inversion [J]. *J. Atmos. Sci.*, 1992, 49: 1397-1411.

Citation: DING Zhi-ying, XING Rui, XU Hai-ming et al. Analysis of effect of environmental potential vorticity located at south edge of South Asia High on intensification of tropical cyclones. *J. Trop. Meteor.*, 2014, 20(1): 74-86.